Receding-horizon pseudospectral control for energy maximization of oscillating-water-column wave energy systems

Marco Rosati[1] and John V. Ringwood[1]

Abstract— **Wave energy, harnessed by wave energy converters (WECs), has the potential to significantly contribute to the renewable energy mix. To improve the commercial viability of WECs, the design of control strategies for maximizing the produced energy is vital. This work specifically focuses on energy maximizing control for oscillating-water-column (OWC) WECs, using a *receding-horizon pseudospectral* (RHPS) optimal control method. With pseudospectral control, the continuous time OWC energy maximizing optimal control problem is *directly transcribed*, by discretizing both state, and control, variables, into a finite-dimensional nonlinear program. Due to the importance of turbine performance, OWC control typically aims to maximize turbine efficiency, albeit ignoring the impact of rotational speed on hydrodynamic performance. With the RHPS optimal control approach developed in this paper, a better trade-off between turbine and hydrodynamic performance is achieved and, therefore, energy production is improved.**

Index Terms— **Optimal control, oscillating-water-column, pseudospectral method, receding-horizon, wave energy.**

I. INTRODUCTION

Wave energy converters (WECs) harness wave energy, which is an almost untapped renewable energy resource that can significantly reduce greenhouse gas emissions [1]. However, in comparison to other renewable resources, the cost of producing energy using waves is relatively high. To improve WECs commercial viability, it is essential to reduce the levelized cost of energy (LCoE), defined as

$$\text{LCoE} = \frac{\text{Capital costs} + \text{Operational costs}}{\text{Produced energy over the WEC lifetime}}, \quad (1)$$

associated with wave energy projects. To this end, the development of energy maximising control strategies is vital [2].

The oscillating-water-column (OWC) system [3], schematically shown in Fig. 1, is one of the most promising WECs due to its relative simplicity of operation, and the fact that all the moving parts are above the water level. The displacement of a water column, due to the excitation force of the ocean waves, compresses/decompresses a volume of air in a pneumatic chamber. The pressure difference, between the pneumatic chamber and the atmosphere, consequently generates a bidirectional air flow, which typically drives a self-rectifying air turbine [4]. Finally, a suitable electric generator converts the turbine mechanical power into electric power.
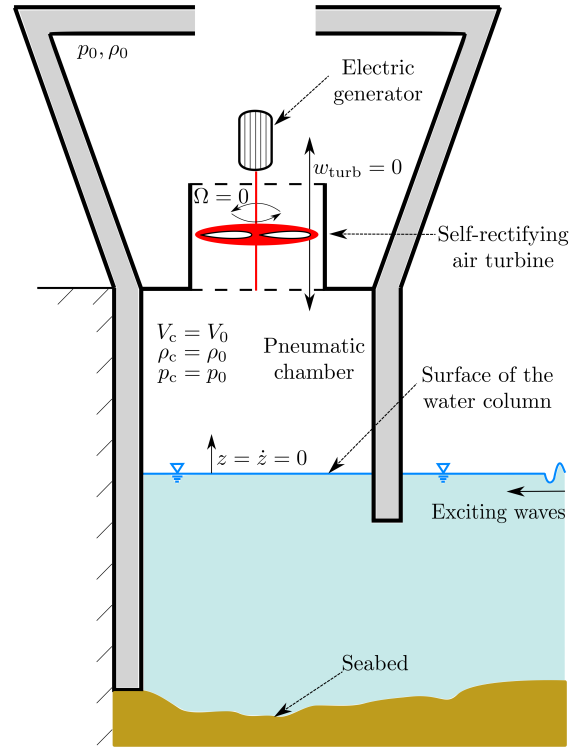
Fig. 1. Schematics of a fixed OWC WEC. Adapted from [5].

To date, since the air turbine is the most critical element of the OWC, and since traditional WEC hydrodynamic control [6] is difficult to apply on OWCs due to the absence of suitable actuators [7], the vast majority of OWC control strategies aim to maximize turbine efficiency [4]. However, for some types of turbines, namely the Wells turbine, rotational speed affects the hydrodynamic performance, particularly when medium-to-high levels of wave energy are available [5]. Therefore, if a Wells turbine is employed, the control strategy should consider also the OWC hydrodynamic characteristics, and not exclusively focus on turbine efficiency. Some works on overall efficiency maximisation for OWCs equipped with a Wells turbine, using a relatively simple and computationally efficient steady-state control approach, have recently emerged [5], [8]. Furthermore, energy maximising control, using nonlinear model predictive control (MPC) [9], [10] and inverse fuzzy model control [11], has been considered for biradial turbines, although the impact of the biradial turbine rotational speed on the OWC hydrodynamic performance is (almost) negligible [5].

This paper develops a *receding-horizon pseudospectral*

(RHPS) optimal control method for energy maximisation of OWC WECs equipped with a Wells turbine (selected for its capability of affecting hydrodynamic efficiency) and an ideal electric generator. A study case, for which a Mutriku-like OWC [12] is considered, shows that the proposed RHPS control improves energy production, in comparison to the traditional turbine efficiency maximising (TEM) control approach. Pseudospectral (PS), or *collocation*, methods belong to a family of techniques, known as mean weighted residuals [13], which are used to discretize integrals and partial differential equations. In particular, PS methods are a subset of the so-called spectral methods, in which state, and control, variables are approximated via a basis function expansion. Although early work on PS optimal control emerged in the late 80s [14], PS control has only found application in more recent years, mainly in flight control [15]. In the wave energy field, PS control has been used to tackle the WEC optimal control problem (OCP) (e.g., [16]–[18]), especially since the discretization in PS methods provides a relatively fast convergence rate [16], resulting in a more computationally efficient nonlinear program (in comparison to MPC [19]), which is potentially suitable for *real-time* applications. Furthermore, the PS representation allows an *analytic* simplification of the radiation convolution integral, which models the radiation force in the WEC hydrodynamic model, as opposed to the somewhat classical approach of using a model reduction technique to approximate the convolution term with a suitable finite-order state space model [20].

The reminder of the paper is organized as follows. In Section II, a complete model for a fixed OWC is provided. In Section III, the proposed RHPS control approach is detailed and the study case is presented. Section IV provides a comprehensive discussion of the results, while conclusions are given in Section V.

II. Oscillating-water-column modelling

This section provides the model of the fixed OWC considered in this paper, which is similar to that employed in [5]. For brevity of notation, the time dependence of variables is omitted throughout the section.

A. Hydrodynamic modelling

A hydrodynamic model for a fixed OWC is specified, under linear potential theory assumptions, as [21]

$$\dot{z} = v$$
$$m_{\mathrm{p}}\dot{v} = -\rho_{\mathrm{w}} g S_{\mathrm{w}} z - S_{\mathrm{w}} \Delta p - f_{\mathrm{r}} + f_{\mathrm{ex}}, \quad (2)$$

where m_{p} is the (neutrally buoyant) water piston mass, S_{w} is the OWC water plane area, ρ_{w} is the water density, g is the gravity acceleration constant, $\Delta p = p_{\mathrm{c}} - p_0$ is the difference between the chamber pressure, p_{c}, and the atmospheric pressure, p_0, z is the water column position, and v is the water column velocity. The wave excitation force, f_{ex}, is calculated as a sum of N_{w} frequency components, ω_{n}, [22] as

$$f_{\mathrm{ex}} = \sum_{\mathrm{n}=1}^{N_{\mathrm{w}}} A_{\mathrm{n}} \cos(\omega_{\mathrm{n}} t + \phi_{\mathrm{n}}), \quad (3)$$

where ϕ_{n} and A_{n} are the phase and amplitude of the n-th component of the excitation force, respectively. Finally, the force due to radiated waves, f_{r}, is written [23] as

$$f_{\mathrm{r}} = A(\infty)\dot{v} + \int_{-\infty}^{t} k_{\mathrm{r}}(t - \tau)\, v(\tau)\, \mathrm{d}\tau, \quad (4)$$

where the piston impulse response function, k_{r}, is the inverse Fourier transform of the OWC radiation damping, $B(\omega)$, and the OWC added mass at infinite frequency, $A(\infty)$, is computed as $A(\infty) = A(\omega)|_{\omega \to \infty}$. WAMIT software [24] is used to solve the boundary element problem [25] and obtain the frequency dependant functions, namely $A(\omega)$, $B(\omega)$, $A_{\mathrm{n}}(\omega)$, and $\phi_{\mathrm{n}}(\omega)$.

B. Pneumatic chamber modelling

The air pressure variation in the pneumatic chamber is modelled [22] as

$$\frac{\dot{p}_{\mathrm{c}}}{p_{\mathrm{c}}} = -\frac{\gamma}{V_{\mathrm{c}}} \left(\frac{\dot{V}_{\mathrm{c}}}{V_{\mathrm{c}}} + \frac{w_{\mathrm{turb}}}{m_{\mathrm{c}}} \right), \quad (5)$$

where γ is the air specific heat ratio, w_{turb} indicates the turbine air mass flow rate (positive for outward air flow), $m_{\mathrm{c}} = \rho_{\mathrm{c}} V_{\mathrm{c}}$ is the air chamber mass, ρ_{c} is the air chamber density, $V_{\mathrm{c}} = V_0 - S_{\mathrm{w}} z$ is the chamber air volume, and V_0 is the air volume in still water conditions. The air compression/expansion is modelled as an isentropic process,

$$\rho_{\mathrm{c}} = \rho_0 \big(\frac{p_{\mathrm{c}}}{p_0}\big)^{1/\gamma}, \quad (6)$$

where ρ_0 is standard atmosphere air density. Finally, the available pneumatic power in the chamber is defined as

$$P_{\mathrm{pneu}} = \Delta p\, w_{\mathrm{turb}} / \rho_{\mathrm{c}}. \quad (7)$$

C. Power take-off system modelling

Under design operating conditions, i.e., large Reynolds (Re $> 10^6$) and low Mach (Ma < 0.3) numbers at the turbine blade tips, the air turbine can be modelled using the following dimensionless description [26]:

$$\Phi = f_{\Phi}(\Psi), \quad \Pi = f_{\Pi}(\Psi), \quad (8)$$

where

$$\Phi = \frac{w_{\mathrm{turb}}}{\rho_{\mathrm{air}}\, \Omega\, d_{\mathrm{r}}^3}, \quad \Pi = \frac{P_{\mathrm{turb}}}{\rho_{\mathrm{air}}\, \Omega^3\, d_{\mathrm{r}}^5}, \quad \Psi = \frac{\Delta p}{\rho_{\mathrm{air}}\, \Omega^2\, d_{\mathrm{r}}^2}. \quad (9)$$

In (8) and (9), Φ is the dimensionless air mass flow rate, Π is the dimensionless turbine power, Ψ is the dimensionless pressure head, Ω is the turbine rotational speed, d_{r} is the turbine rotor diameter, P_{turb} is the turbine power, and $\rho_{\mathrm{air}} = \min(\rho_{\mathrm{c}}, \rho_0)$ is the air density at the turbine inlet. Finally, the turbine efficiency is defined as

$$\eta_{\mathrm{turb}}(\Psi) = \frac{P_{\mathrm{turb}}}{P_{\mathrm{pneu}}} = \frac{f_{\Pi}(\Psi)}{\Psi\, f_{\Phi}(\Psi)}, \quad (10)$$

The dimensionless functions $f_{\Phi}(\Psi)$, $f_{\Pi}(\Psi)$, and $\eta_{\mathrm{turb}}(\Psi)$, for the Wells turbine considered in this paper, are shown in Fig. 2.
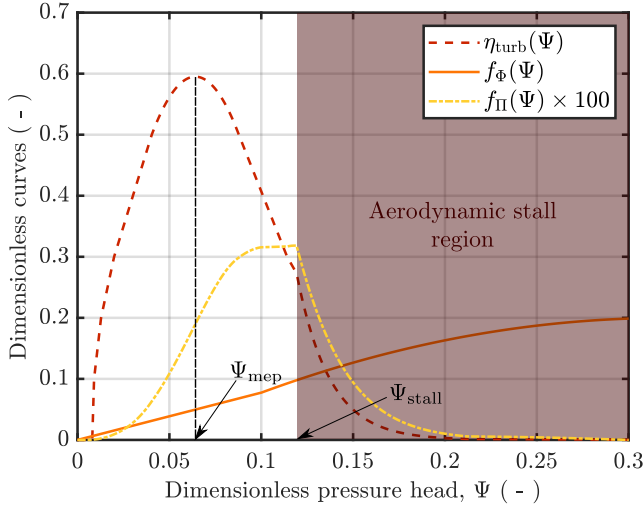
Fig. 2. Model of the Wells turbine considered in this work [5]. The figure shows the turbine efficiency, η_{turb}, dimensionless flow rate, Φ, and dimensionless power, Π, as functions of the dimensionless pressure head, Ψ. Ψ_{mep} is Ψ at the turbine maximum efficiency point (MEP).

Fig. 3. Relationship between the pressure difference, Δp, and the air mass flow rate, w_{turb}, as Ω changes, for a Wells turbine and a biradial turbine. Figure adapted from [5].

If bearing friction losses are ignored, the PTO system dynamic is modelled as

$$\frac{\mathrm{d}}{\mathrm{d}t}\left(\frac{1}{2}I\Omega^2\right) = P_{\text{turb}} - T_{\text{ctrl}}\,\Omega, \tag{11}$$

where I is the inertia moment of the rotating parts, P_{turb} is the turbine mechanical power, computed using (8) and (9), and T_{ctrl} is the generator control torque.

Turbine damping, ζ, is defined as the ratio $w_{\text{turb}}/\Delta p$. In impulse-like turbines, ζ only marginally depends on Ω [27], meaning that the OWC hydrodynamic performance is not significantly affected by the rotational speed. However, the Wells turbine damping is a function of Ω [28], as

$$\zeta = \frac{w_{\text{turb}}}{\Delta p} = \frac{d_{\text{r}}}{\kappa\,\Omega}, \tag{12}$$

where κ is a constant that depends on the turbine geometry. With a Wells turbine, it is therefore possible to potentially improve the OWC hydrodynamic performance by modulating Ω. Fig. 3 shows the relationship between w_{turb} and Δp, as Ω varies, for a Wells turbine and a biradial turbine.

III. Receding horizon pseudospectral control

With PS optimal control, the original infinite-dimensional OWC OCP is directly transcribed (e.g., [29]), meaning that the associated state, and input, variables are suitably discretized, into a finite-dimensional nonlinear program.

A. Pseudospectral representation

To illustrate pseudospectral optimal control, consider the generic dynamical system

$$\dot{\mathbf{x}} = \mathbf{f}(\mathbf{x}(t), \mathbf{u}(t), t)\ t \in [0, T], \tag{13}$$

with state vector $\mathbf{x}(t) \in \mathbb{R}^n$, control input vector $\mathbf{u}(t) \in \mathbb{R}^m$, and $\mathbf{f} : \mathbb{R}^n \times \mathbb{R}^m \times \mathbb{R} \to \mathbb{R}^n$. Additionally, suppose that
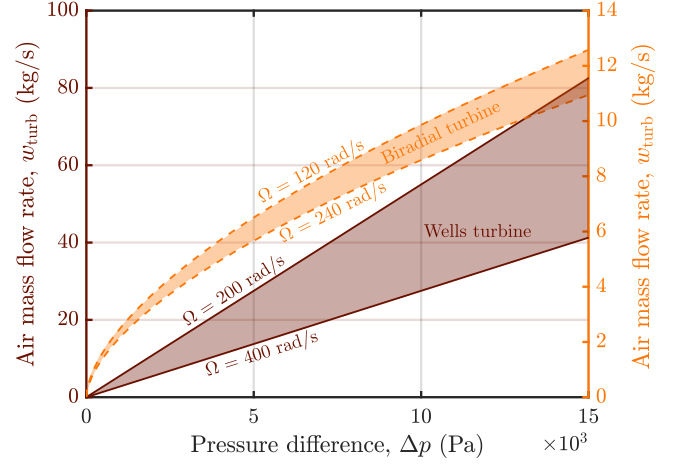
the OCP is to find the optimal control input, $\mathbf{u}^{\text{opt}}$, which maximises (or minimises) the following cost functional:

$$J = \int_0^T h(\mathbf{x}(t), \mathbf{u}(t), t)dt,\ h : \mathbb{R}^n \times \mathbb{R}^m \times \mathbb{R} \to \mathbb{R}^n \tag{14}$$

subject to the system dynamic in (13).

The i-th component of $\mathbf{x}(t)$ $(i = 1, \ldots n)$ and the j-th component of $\mathbf{u}(t)$ $(j = 1, \ldots m)$ are approximated via an expansion of M basis functions, $\theta_{\text{q}}(t)$, as

$$x_{\text{i}}(t) \approx x_{\text{i}}^{\text{M}}(t) := \sum_{\text{q}=1}^{\text{M}} \tilde{x}_{\text{iq}}\theta_{\text{q}}(t) = \Theta(t)\hat{\mathbf{x}}_{\text{i}}, \tag{15}$$

and

$$u_{\text{j}}(t) \approx u_{\text{j}}^{\text{M}}(t) := \sum_{\text{q}=1}^{\text{M}} \tilde{u}_{\text{jq}}\theta_{\text{q}}(t) = \Theta(t)\hat{\mathbf{u}}_{\text{j}}, \tag{16}$$

respectively, where

$$\Theta(t) = [\theta_1(t), \ldots \theta_{\text{q}}(t), \ldots \theta_{\text{M}}(t)] \tag{17}$$

and

$$\begin{aligned} \hat{\mathbf{x}}_{\text{i}} &= [\tilde{x}_{\text{i1}}, \ldots \tilde{x}_{\text{iq}}, \ldots \tilde{x}_{\text{iM}}]^{\mathsf{T}}, \\ \hat{\mathbf{u}}_{\text{j}} &= [\tilde{u}_{\text{j1}}, \ldots \tilde{u}_{\text{jq}}, \ldots \tilde{u}_{\text{jM}}]^{\mathsf{T}}. \end{aligned} \tag{18}$$

To simplify the notation, it is useful to introduce the matrices $\mathbf{X} \in \mathbb{R}^{M \times n}$ and $\mathbf{U} \in \mathbb{R}^{M \times m}$, respectively, as

$$\mathbf{X} = [\hat{\mathbf{x}}_1, \ldots \hat{\mathbf{x}}_{\text{i}}, \ldots \hat{\mathbf{x}}_{\text{n}}] \text{ and } \mathbf{U} = [\hat{\mathbf{u}}_1, \ldots \hat{\mathbf{u}}_{\text{j}}, \ldots \hat{\mathbf{u}}_{\text{m}}]. \tag{19}$$

Due to the approximations (15) and (16), since the cost functional (14) solely depends on the $M(n+m)$ parameters of $\mathbf{X}$ and $\mathbf{U}$, the OCP is now finite-dimensional.

If (15), (16), and

$$\dot{x}_{\text{i}}(t) \approx \dot{x}_{\text{i}}^{\text{M}}(t) := \sum_{\text{q}=1}^{\text{M}} \tilde{x}_{\text{iq}}\dot{\theta}_{\text{q}}(t) = \dot{\Theta}(t)\hat{\mathbf{x}}_{\text{i}}, \tag{20}$$

are replaced in (13), the i-th dynamic equation in residual form can be written, as

$$r_{\mathrm{i}}(t) = \dot{x}_{\mathrm{i}}^{\mathrm{M}}(t) - f_{\mathrm{i}}(\mathbf{x}^{\mathrm{M}}(t), \mathbf{u}^{\mathrm{M}}(t), t), \tag{21}$$

where $\mathbf{x}^{\mathrm{M}}$ and $\mathbf{u}^{\mathrm{M}}$ are the vectors of the approximated n state variables (in (15)) and m control inputs (in (16)), respectively. To obtain the $M(n + m)$ parameters (i.e., $\hat{\mathbf{x}}_{\mathrm{i}}$ and $\hat{\mathbf{u}}_{\mathrm{j}}$ in (18)), which minimise the n residuals in (21), a pseudospectral, or collocation, method can be adopted. To this end, a number, N_{c}, of collocation points (or nodes), t_{k}, upon which the system dynamic is 'collocated', are selected. In other words, the system dynamic equation is satisfied at the collocation points, meaning that the residuals are zero at the N_{c} nodes:

$$r_{\mathrm{i}}(t_{\mathrm{k}}) = \dot{\Theta}(t_{\mathrm{k}})\hat{\mathbf{x}}_{\mathrm{i}} - f_{\mathrm{i}}(\mathbf{X}, \mathbf{U}, t_{\mathrm{k}}) = 0. \tag{22}$$

Finally, a suitable quadrature formula approximates the functional in (14), as

$$J = \int_0^T h(\mathbf{X}, \mathbf{U}, t)dt \approx \sum_{\mathrm{k}=0}^{N_{\mathrm{c}}} h(\mathbf{X}, \mathbf{U}, t_{\mathrm{k}}). \tag{23}$$

The original optimal control problem, namely find $\mathbf{u}^{\mathrm{opt}}$ that minimises (or maximises) (14) subject to (13), is simplified to the following finite dimensional optimisation problem: Find $\mathbf{X}$ and $\mathbf{U}$ to minimise (or maximise) (23) subject to the equality constraints due to the system dynamic (22), which is a system of $n \times N_{\mathrm{c}}$ equations (n state variables and N_{c} nodes).

B. Pseudospectral optimal control for OWCs

For the OWC considered in this paper, the state vector and control input are specified, respectively, as

$$\mathbf{x}(t) = [z(t) \; v(t) \; \Delta p(t) \; \Omega(t)]^{\mathsf{T}} \text{ and } u(t) = T_{\mathrm{ctrl}}(t). \tag{24}$$

Furthermore, the control objective is to maximise mechanical energy

$$J = \int_0^T T_{\mathrm{ctrl}}(t) \, \Omega(t) \, dt, \; t \in [0 \; T] \tag{25}$$

subject to the constraints given by the OWC system dynamic in (2), (5), and (11). Given the oscillatory nature of the problem, a somewhat natural choice of basis functions is that of a truncated Fourier series (zero-mean trigonometric polynomial), therefore

$$x_{\mathrm{i}}(t) \approx \sum_{\mathrm{q}=1}^{\mathrm{M}} x_{\mathrm{iq}}^{\mathrm{c}}\cos(q\omega_0 t) + x_{\mathrm{iq}}^{\mathrm{s}}\sin(q\omega_0 t) = \Theta(t)\hat{\mathbf{x}}_{\mathrm{i}}$$

$$u(t) \approx \sum_{\mathrm{q}=1}^{\mathrm{M}} u_{\mathrm{q}}^{\mathrm{c}}\cos(q\omega_0 t) + u_{\mathrm{q}}^{\mathrm{s}}\sin(q\omega_0 t) = \Theta(t)\hat{\mathbf{u}}, \tag{26}$$

where $\omega_0 = 2\pi/T$ is the fundamental frequency. By substituting (26) into (25), the cost function becomes

$$J = \int_0^T \hat{\mathbf{u}}^{\mathsf{T}}\Theta(t)^{\mathsf{T}}\Theta(t)\hat{\mathbf{x}}_4 \, dt = \frac{T}{2}\hat{\mathbf{u}}^{\mathsf{T}}\hat{\mathbf{x}}_4, \tag{27}$$

due to the orthogonality of Θ, i.e., $\langle \theta_{\mathrm{q}}, \theta_{\mathrm{p}} \rangle = \delta_{\mathrm{qp}}T/2$ (where δ_{qp} is the Kronecker delta). To investigate real-time

control possibilities, this paper considers a receding-horizon approach to tackle the OWC OCP. Therefore, T in (27) is replaced with the length of the prediction horizon, T_{h}.

The derivative of the i-th approximated state variable is

$$\dot{x}_{\mathrm{i}}^{\mathrm{M}} = \dot{\Theta}(t)\hat{\mathbf{x}}_{\mathrm{i}} = \Theta(t)D_{\theta}\hat{\mathbf{x}}_{\mathrm{i}}, \tag{28}$$

where the q-th block of the block diagonal matrix, $D_{\theta} \in \mathbb{R}^{2M \times 2M}$, is

$$D_{\theta}^{\mathrm{q}} = \begin{bmatrix} 0 & q\omega_0 \\ -q\omega_0 & 0 \end{bmatrix}. \tag{29}$$

By use of (26) and (29), the system dynamic equations (i.e., (2), (5), and (11)), in residual form, and collocated at N_{c} uniformly spaced nodes t_k (with N_{c} sufficiently large), are expressed as

$$r_1 = D_{\theta}\hat{\mathbf{x}}_1 - \hat{\mathbf{x}}_2,$$
$$r_2(t_k) = m_{\mathrm{p}}\Theta(t_k)D_{\theta}\hat{\mathbf{x}}_2 + \rho_{\mathrm{w}}gS_{\mathrm{w}}\Theta(t_k)\hat{\mathbf{x}}_1$$
$$\quad + S_{\mathrm{w}}\Theta(t_k)\hat{\mathbf{x}}_3 + \Theta(t_k)G\hat{\mathbf{x}}_2 - f_{\mathrm{ex}}(t_k),$$
$$r_3(t_k) = \Theta(t_k)D_{\theta}\hat{\mathbf{x}}_3 + (\Theta(t_k)\hat{\mathbf{x}}_3 + p_0)\frac{\gamma}{V_0 - S_{\mathrm{w}}\Theta(t_k)\hat{\mathbf{x}}_1}$$
$$\quad \left(-S_{\mathrm{w}}\Theta(t_k)\hat{\mathbf{x}}_2 + \frac{d_{\mathrm{r}}}{\rho_c\kappa}\frac{\Theta(t_k)\hat{\mathbf{x}}_3}{\Theta(t_k)\hat{\mathbf{x}}_4}\right),$$
$$r_4(t_k) = \Theta(t_k)D_{\theta}\hat{\mathbf{x}}_4 - (\rho_{\mathrm{air}}d_{\mathrm{r}}^5 f_{\Pi}\Theta(t_k)\hat{\mathbf{x}}_3\Theta(t_k)\hat{\mathbf{x}}_3$$
$$\quad - \Theta(t_k)\hat{\mathbf{u}})/I. \tag{30}$$

The matrix $G \in \mathbb{R}^{2M \times 2M}$, which results from the approximation of the convolution integral in the PS formulation (e.g., [16]), specified from

$$\int_{-\infty}^t k_{\mathrm{r}}(t_k - \tau)x_2^{\mathrm{M}}(\tau)\mathrm{d}\tau = \Theta(t_k)(G - A(\infty)D_{\theta})\hat{\mathbf{x}}_2, \tag{31}$$

is a block diagonal matrix, and the q-th block of G is

$$G^{\mathrm{q}} = \begin{bmatrix} B(q\omega_0) & q\omega_0 A(q\omega_0) \\ -q\omega_0 A(q\omega_0) & B(q\omega_0) \end{bmatrix}. \tag{32}$$

C. Study case description

For the study case, the proposed RHPS control is numerically tested on a Mutriku-like OWC WEC, whose design parameters are reported in Table I, and compared to the traditional TEM control approach [30]. A representative irregular sea state [5], obtained from a JONSWAP spectral density function [31], with peak shape parameter $\gamma^J = 3.3$, peak period, $T_{\mathrm{p}} = 10$ s, and significant wave height, $H_{\mathrm{s}} = 1.08$ m, is used in the simulation.

To explore real-time control possibilities, four different prediction horizons are considered (namely, $T_{\mathrm{h}} = 5, 10, 15$, and 20 seconds) and the receding-horizon time step, Δ_{rh}, is 0.5 s. For each considered T_{h}, 20 realisations of 300 s are run with $M = 20$. In a receding-horizon framework, the use of Fourier series to approximate non-periodic functions gives a discontinuity problem at the boundary, known as Gibbs phenomenon. In this paper, the solution proposed in [32], which is based on the construction of a buffer zone using a smooth polynomial function, is adopted to avoid such discontinuities. Finally, the optimisation problem is solved

TABLE I

OWC SYSTEM PARAMETERS

Parameter	Value	Unit	Parameter	Value	Unit
m_{p}	27748	kg	I	3.06	kg m^2
$A(\infty)$	71618	kg	κ	0.775	-
l	4.5	m	V_0	144	m^3
d_{r}	0.75	m	S_{w}	19.35	m^2

TABLE II

RESULTS FOR DIFFERENT PREDICTION HORIZONS

Prediction horizon (s)	Turbine efficiency (%)	Hydro. CWR (%)	Aero. CWR (%)	Power increase (%)	Comp. time* (s)
5 ($0.5T_{\mathrm{p}}$)	35.9	53.5	19.2	5.7	0.17
10 ($1.0T_{\mathrm{p}}$)	35.3	56.4	19.9	9.3	0.43
15 ($1.5T_{\mathrm{p}}$)	36.2	56.5	20.5	11.7	0.89
20 ($2.0T_{\mathrm{p}}$)	36.4	57.1	20.8	12.9	1.54

*Using a PC with a core i7-12700 processor and a 32 GB RAM.

using an interior-point method [33], due to its capability of dealing with large sparse matrices.

IV. RESULT AND DISCUSSION

A. Results

Table II reports the turbine efficiency, hydrodynamic capture width ratio (CWR), ξ_{hydro}, aerodynamic CWR, ξ_{aero}, and mean computational time to solve the optimisation problem, for four different prediction horizons. The hydrodynamic CWR and aerodynamic CWR are defined, respectively, as

$$\xi_{\mathrm{hydro}} = \frac{\bar{P}_{\mathrm{pneu}}}{\bar{P}_{\mathrm{wave}}\, l}, \; \xi_{\mathrm{aero}} = \frac{\bar{P}_{\mathrm{turb}}}{\bar{P}_{\mathrm{wave}}\, l}, \qquad (33)$$

where l is the OWC width, $\bar{P}_{\mathrm{wave}}$ is the time-averaged wave power per metre of wave crest, while $\bar{P}_{\mathrm{pneu}}$ and $\bar{P}_{\mathrm{turb}}$ are, respectively, the time-averaged pneumatic and turbine powers. Furthermore, Table II also shows the percentage increase in mechanical power obtained using RHPS control, in comparison to TEM control.

Figures 4 (a) and (b) show, respectively, the time traces of the rotational speed and control torque, under TEM control and RHPS control (with $T_{\mathrm{h}} = 10$ s). Finally, Fig. 5 shows the computational time required to solve each optimisation problem, for $T_{\mathrm{h}} = 5$ s and $T_{\mathrm{h}} = 10$ s, as a function of the simulation time.

B. Discussion

For all the considered prediction horizons in Table II, the power increase obtained with RHPS control, compared to TEM control, is due to the fact that a better trade-off between the hydrodynamic and aerodynamic performance is achieved, meaning that a higher ξ_{aero} is attained. With TEM control, the turbine efficiency, hydrodynamic CWR, and aerodynamic CWR are 37.7%, 45.8%, and 17.3%, respectively. Therefore, although $\bar{\eta}_{\mathrm{turb}}$ is higher with TEM control, RHPS control better considers the impact of Ω on the OWC hydrodynamic subsystem and, consequently, ξ_{hydro} is superior, particularly since RHPS control generates larger pressure peaks (due to
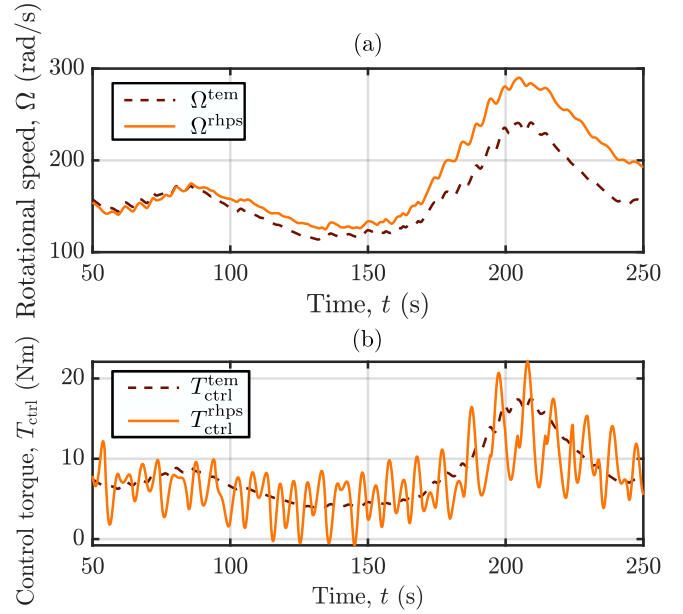

Fig. 4. Time series of the (a) rotational speed, Ω, and (b) control torque, T_{ctrl}, with the traditional TEM control and RHPS optimal control.
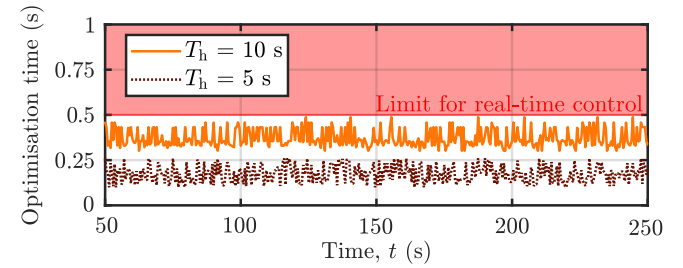

Fig. 5. Time required to solve each optimisation problem, as a function of the simulation time, for two different prediction horizons, namely $T_{\mathrm{h}} = 5$ s and $T_{\mathrm{h}} = 10$ s. The red line at 0.5 s indicates the computational time limit for real-time control.

the pulses in $T_{\mathrm{ctrl}}^{\mathrm{rhps}}$, and therefore in Ω) which, in turns, lead to higher pneumatic power.

As reported in Table II, as T_{h} increases, power production improves at the cost of a higher computational burden. For real-time control (considering the PC specified in the footnote of Table II), only $T_{\mathrm{h}} = 5$ s and $T_{\mathrm{h}} = 10$ s can be used, since each optimisation problem is consistently solved in less than 0.5 s (as shown in Fig. 5), which is the limit for real-time control (i.e., $T_{\mathrm{comp}} < \Delta_{\mathrm{rh}}$).

It is important to note that, in contrast to TEM control, RHPS control may require negative control torque values (as shown in Fig. 4(b)), meaning that reactive power must be provided to the OWC system to maximise energy. The need for supplying reactive power to maximize wave energy extraction is not unusual in traditional WEC (hydrodynamic) control [6]; however, it remains significantly more challenging for OWCs, primarily due to the lack of suitable actuators [7]. In light of Fig. 4(b), the reactive power required on OWCs is significantly lower than the amount of reactive power typically required in energy maximising control for

other WEC types. This is arguably due to the presence of a 'soft connection' (i.e., the air chamber) between the PTO and the OWC hydrodynamic part, meaning that: (i) the OWC PTO is not constrained to always move in concert with the ocean waves [4], and (ii) the degree to which rotational speed modulation affects hydrodynamic performance in OWCs is limited, particularly in comparison to what traditional WEC (hydrodynamic) control can do on other WEC types.

V. Conclusions

For T_h = 10 s and T_h = 5 s, the proposed RHPS control offers a relatively computationally efficient solution to the OWC OCP and, in comparison with the traditional TEM control, improves energy production since the hydrodynamic performance is better taken into account.

For real-time PS control, a receding-horizon approach is essential, although the prediction horizon length is limited by the available computational power, as well as by the errors in the excitation force prediction which may deteriorate control performance [34].

It should be noted that the higher harmonics in $T_\mathrm{ctrl}^\mathrm{rhps}$ (Figure 4(b)) may increase OpEx and, therefore, the LCoE. However, the most detrimental effect on OWC is turbine stall, which generates high frequency vibrations [35], and, to this end, RHPS control tends to keep Ω higher (Figure 4(a)), hence reducing the risk of stall.

References

[1] S. Astariz and G. Iglesias, "The economics of wave energy: A review," *Renew. Sust. Energ. Rev.*, vol. 45, pp. 397–408, 2015.

[2] G. Chang, C. A. Jones, J. D. Roberts, and V. S. Neary, "A comprehensive evaluation of factors affecting the levelized cost of wave energy conversion projects," *Renew. Energy*, vol. 127, pp. 344–354, 2018.

[3] A. F. O. Falcão and J. C. C. Henriques, "Oscillating-water-column wave energy converters and air turbines: A review," *Renew. Energy*, vol. 85, pp. 1391–1424, 2016.

[4] M. Rosati, J. C. C. Henriques, and J. V. Ringwood, "Oscillating-water-column wave energy converters: A critical review of numerical modelling and control," *Energy Convers. Manag. X*, vol. 16, p. 100322, 2022.

[5] M. Rosati and J. V. Ringwood, "Wave-to-wire efficiency maximisation for oscillating water column systems," in *Proc. of the 22nd IFAC World Congress*, Yokohama, Japan, 2023.

[6] J. V. Ringwood, "Wave energy control: Status and perspectives 2020," in *Proc. of the 21st IFAC World Congress*, Berlin, Germany, 2020.

[7] M. Rosati and J. V. Ringwood, "Towards hydrodynamic control of an oscillating water column wave energy converter," *Trends in Renew. Energ. Offshore*, pp. 411–418, 2022.

[8] M. Rosati, H. A. Said, and J. V. Ringwood, "Wave-to-wire control of an oscillating water column wave energy system equipped with a wells turbine," in *Proc. of the 15th European Wave and Tidal Energy Conference*, Bilbao, Spain, 2023, pp. 1–9.

[9] M. E. Magaña, C. Parlapanis, D. T. Gaebele, and O. Sawodny, "Maximization of wave energy conversion into electricity using oscillating water columns and nonlinear model predictive control," *IEEE Trans. Sustai.*, vol. 13, no. 3, pp. 1283–1292, 2022.

[10] J. Marques Silva, S. M. Vieira, D. Valério, and J. C. C. Henriques, "Model predictive control based on air pressure forecasting of OWC wave power plants," *Energy*, 2023.

[11] J. M. Silva, S. M. Vieira, D. Valério, and J. C. C. Henriques, "GA-optimized inverse fuzzy model control of OWC wave power plants," *Renew. Energy*, vol. 204, pp. 556–568, 2023.

[12] Y. Torre-Enciso, I. Ortubia, L. I. L. De Aguileta, and J. Marqués, "Mutriku wave power plant: From the thinking out to the reality," in *Proc. of the 8th European Wave and Tidal Energy Conference*, Uppsala, Sweden, 2009, pp. 319–329.

[13] B. Fornberg, *A Practical Guide to Pseudospectral Methods*. Cambridge University Press, 1996.

[14] J. Vlassenbroeck and R. Van Dooren, "A chebyshev technique for solving nonlinear optimal control problems," *IEEE Trans. Automat. Contr*, vol. 33, no. 4, pp. 333–340, 1988.

[15] I. M. Ross and M. Karpenko, "A review of pseudospectral optimal control: From theory to flight," *Annu. Rev. Control.*, vol. 36, no. 2, pp. 182–197, 2012.

[16] G. Bacelli and J. V. Ringwood, "Nonlinear optimal wave energy converter control with application to a flap-type device," in *Proc. of the 19th IFAC World Congress*, vol. 47, Cape Town, South Africa, 2014, pp. 7696–7701.

[17] R. Genest and J. V. Ringwood, "Receding horizon pseudospectral control for energy maximization with application to wave energy devices," *IEEE Trans. Control Syst. Technol.*, vol. 25, no. 1, pp. 29–38, 2016.

[18] N. M. Tom, Y.-H. Yu, A. D. Wright, and M. J. Lawson, "Pseudo-spectral control of a novel oscillating surge wave energy converter in regular waves for power optimization including load reduction," *Ocean Eng.*, vol. 137, pp. 352–366, 2017.

[19] R. Genest and J. V. Ringwood, "A critical comparison of model-predictive and pseudospectral control for wave energy devices," *J. Ocean Eng. Mar. Energy*, vol. 2, pp. 485–499, 2016.

[20] Y. Peña-Sanchez, N. Faedo, and J. V. Ringwood, "A critical comparison between parametric approximation methods for radiation forces in wave energy systems," in *Proc. of the 29th International Ocean and Polar Engineering Conference*, Honolulu, USA, 2019.

[21] D. V. Evans, "The oscillating water column wave-energy device," *IMA J. Appl. Math.*, vol. 22, no. 4, pp. 423–433, 1978.

[22] J. C. C. Henriques, J. C. C. Portillo, W. Sheng, L. M. C. Gato, and A. F. O. Falcão, "Dynamics and control of air turbines in oscillating-water-column wave energy converters: Analyses and case study," *Renew. Sust. Energ. Rev.*, vol. 112, pp. 571–589, 2019.

[23] W. E. Cummins, "The impulse response function and ship motions," *Schiffstechnik*, pp. 101–109, 1962.

[24] J. N. Ewman and C. H. Lee, "WAMIT user manual," 2016, last accessed 02 March 2019. [Online]. Available: http://www.wamit.com/manual.htm

[25] J. Falnes, *Wave Interaction with Oscillating Water Columns*. Cambridge University Press, 2002, p. 225–262.

[26] S. L. Dixon and C. Hall, *Fluid Mechanics and Thermodynamics of Turbomachinery*. Butterworth-Heinemann, 2013.

[27] M. Rosati, J. V. Ringwood, and J. C. C. Henriques, "A comprehensive wave-to-wire control formulation for oscillating water column wave energy converters," *Trends in Renew. Energ. Offshore*, pp. 329–337, 2022.

[28] A. F. O. Falcão and L. M. C. Gato, "Air turbines," in *Comprehensive Renew. Energ.*, A. Sayigh, Ed. Oxford: Elsevier, 2012, vol. 8, pp. 111–149.

[29] O. Von Stryk, *Numerical Solution of Optimal Control Problems by Direct Collocation*. Springer, 1993.

[30] P. A. P. Justino and A. F. O. Falcão, "Rotational Speed Control of an OWC Wave Power Plant," *J. Offshore Mech. Arct. Eng.*, vol. 121, no. 2, pp. 65–70, 1999.

[31] K. Hasselmann, T. P. Barnett, E. Bouws, H. Carlson, D. E. Cartwright, K. Enke, J. A. Ewing, A. Gienapp, D. E. Hasselmann, P. Kruseman *et al.*, "Measurements of wind-wave growth and swell decay during the joint north sea wave project (JONSWAP)." *Deutches Hydrographisches Institut*, 1973.

[32] H. Fu and C. Liu, "A buffered Fourier spectral method for non-periodic PDE," *Int. J. Numer. Anal.*, vol. 9, no. 2, 2012.

[33] R. A. Waltz, J. L. Morales, J. Nocedal, and D. Orban, "An interior algorithm for nonlinear optimization that combines line search and trust region steps," *Math. Program.*, vol. 107, no. 3, pp. 391–408, 2006.

[34] B. Guo, R. J. Patton, S. Jin, and J. Lan, "Numerical and experimental studies of excitation force approximation for wave energy conversion," *Renew. Energ.*, vol. 125, pp. 877–889, 2018.

[35] D. L. Bruschi, J. C. S. Fernandes, A. F. O. Falcão, and C. P. Bergmann, "Analysis of the degradation in the Wells turbine blades of the Pico oscillating-water-column wave energy plant," *Renew. Sust. Energ. Rev.*, vol. 115, 2019.